A Theoretical and Experimental Study of the Electron Spin Resonance of a Number of Low Symmetry Copper(II) Dimers

By **Peter D. W. Boyd, A. David Toy,** and **Thomas D. Smith,*** Chemistry Department, and **John R. Pilbrow,** Physics Department, Monash University, Clayton, Victoria, Australia 3168

Theoretical considerations of the interactions in pair systems of identical copper(II) ions have shown that the symmetry of the pair system plays an important role in determining the form of the zero-field splitting appropriate to the triplet state e.s.r. spectra observed in such circumstances. To test the theoretical predictions, a number of compounds, for which *X*-ray structural evidence was available, have been studied either as powders, doped into isomorphous diamagnetic hosts, or in suitable solvents. The particular systems studied are copper(II) complexes of diethyldithiocarbamate, pyridine *N*-oxide, salicylaldehyde, and tartaric acid. These examples involve dimeric units such that the overall dimer symmetry is monoclinic. Theoretical results are discussed in the limit of weak exchange coupling, small compared with the *X*-band microwave energy, as well as for exchange coupling large compared with *X*-band energy but not greater than *ca.* 30 cm^{-1}. Within these limits, the zero-field splitting which manifests itself in the e.s.r. spectrum, is believed to be due entirely to dipole–dipole coupling between the copper(II) pairs. A perturbation theory approach leads to analytical expressions for transition field positions and intensities which are then used in the computer simulation of spectra. Excellent agreement is found between *X*-ray and e.s.r. structural parameters, except for the tartrate which is thought to possess a different dimer structure in frozen solution than in the pure copper compound.

RECENT development in the interpretation of e.s.r. spectra due to paramagnetic dimers by means of computer simulation of the spectra based on a model which assumes dipole–dipole coupling of the ions, has provided a convenient method for the determination of the internuclear separation of the metal ions.[1-3] This information has proved useful in the elucidation of the structure of binuclear or dimeric forms of metal ion chelate systems. So far, the theoretical treatment has been restricted to the assumption of axial symmetry for the pair system. Crystallographic studies of dimeric metal chelates, as well as consideration of the stereochemical requirements of certain ligands clearly indicate that other symmetry arrangements of the pair of paramagnetic ions will occur. Thus in order to account adequately for the experimental e.s.r. spectra observed in such circumstances, and to extract the internuclear distance between the metal ion pairs in a meaningful way, the effect of symmetry on the magnetic interactions in the pairs of ions of spin $\frac{1}{2}$ has been considered. Although the examples presented later all involve copper(II) pairs, the theory applies equally well to other pairs of ions with spin $\frac{1}{2}$, and in particular to titanium(III) or vanadyl ion pairs.

The various symmetry arrangements to be discussed here are represented by the co-ordinate diagram, Figure 1. It is assumed that the two paramagnetic ions (1 and 2) are in identical sites of orthorhombic symmetry, and where the *g* and *A* (hyperfine) tensor principal axes for 1 and 2 are all parallel. To clarify the situation the various symmetry types covered by the model are summarised in Table 1. Some minor modification to the present theory would be necessary when the dimer does not possess inversion symmetry.

Of principal concern in this paper is the second to last situation in Table 1, that for which the dimer symmetry is monoclinic. To test the results in this case, we later compare theoretical and experimental spectra for a number of copper(II) systems where there is a certain amount of *X*-ray structural data available.

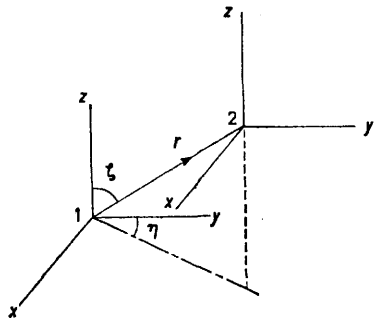

FIGURE 1 Orientation of *g* tensor principal axes and internuclear axis for centrosymmetric metal ion dimers

These are copper(II) diethyldithiocarbamate, doped into the corresponding zinc compound, copper complexes with pyridine *N*-oxide, salicylaldehyde, and tartaric acid. We also make some comparison with the results expected in general if the dimer symmetry is triclinic.

TABLE 1

Symmetry of centrosymmetric dimers

ξ^0	η^0	*g* Tensor and *A* tensor	Dimer symmetry
0	0	Axial	Axial
0	0	Orthorhombic	Orthorhombic
90	0	Axial or orthorhombic	Orthorhombic
$\neq 0$	0	Axial or orthorhombic	Monoclinic
$\neq 0$	$\neq 0$	Orthorhombic	Triclinic

To assist the reader in following the essential features of the derivation, we summarise the procedure in the flow diagram given as Table 2. In view of the extent of the calculations, some of the detail is relegated to the Appendix.

The theory is a variation on the familiar singlet–triplet problem, complicated by *g* and *A* anisotropy

[1] R. H. Dunhill, J. R. Pilbrow, and T. D. Smith, *J. Chem. Phys.*, 1966, **45**, 1474.

[2] J. F. Boas, R. H. Dunhill, J. R. Pilbrow, R. C. Srivastava, and T. D. Smith, *J. Chem. Soc.* (*A*), 1969, 94; T. D. Smith, T. Lund, and J. R. Pilbrow, *ibid.*, 1971, 2786; T. D. Smith, T. Lund, J. R. Pilbrow, and J. H. Price, *ibid.*, 1971, 2936.

[3] J. H. Price, J. R. Pilbrow, K. S. Murray, and T. D. Smith, *J. Chem. Soc.* (*A*), 1970, 968.

as well as by the low symmetry considerations. In general, because of both dipolar and hyperfine terms, *the states* are not pure singlets or triplets which means that the problem does not reduce simply to the paramagnetic triplet state except when the exchange energy is appreciable. We write 'singlet' and 'triplet' to indicate that there are in fact $(2I_1 + 1)(2I_2 + 1) = 16$ such sets of states due to the presence of the copper hyperfine interaction. [$I_1 = 3/2$ and $I_2 = 3/2$ are the nuclear spins of the two copper(II) ions.] The energy levels and wavefunctions derived later have an explicit dependence upon the nuclear quantum numbers (to be defined later) for the two interacting ions.

As will be clear from Table 2, energy levels and wavefunctions of the pair system are worked out by means

TABLE 2

Flow diagram for calculations and computer simulation of spectra

Consider dipole–dipole exchange terms for triclinic dimer symmetry

↓

Energy matrix in a magnetic field

↓

Diagonalise part of energy matrix → 'singlet,' 'triplet.' (Ignore least important hyperfine terms at this stage)

↓

Assume Zeeman interaction ≫ dipolar; include *all* hyperfine terms. Calculate energy levels to *second* order, wavefunctions to *first* order in dipolar and hyperfine effects

↓

Derive transition fields and intensities for $\Delta M = 1$ and 2 transitions

↓

Consider effect of size of J:

$|J| \ll h\nu$(microwave energy): require all energy levels
$|J| \gg h\nu$: e.s.r. 'triplet' problem only
$|J| \approx h\nu$: complications discussed

↓

Simulation of theoretical spectra

↓

Comparison of simulated and experimental spectra

↓

Comparison of e.s.r. and *X*-ray data

of standard perturbation theory. It is not practicable at the present time to consider computer diagonalisation methods in view of the many times such large matrices, 64 × 64, for copper(II) pairs would have to be diagonalised in order to enable a computer simulation of the spectra to be carried out. Furthermore as may be judged from the agreement between theoretical and experimental spectra later in this paper, such an approach does not seem necessary for the present systems.

THEORY OF $S = \frac{1}{2}$ DIMERS IN A MAGNETIC FIELD

Symmetry and the Zero Field Splitting Tensor.—The interaction between two identical ions with Kramers doublet ground states ($S_1 = S_2 = \frac{1}{2}$) may be represented by the effective spin Hamiltonian as the sum of two terms [4]

$$\mathscr{H}_{\text{int}} = -J\mathbf{S}_1 \cdot \mathbf{S}_2 + \mathbf{S}_1 \cdot \mathscr{J} \cdot \mathbf{S}_2 \qquad (1)$$

In equation (1), the first term arises from exchange, and is a scalar coupling, while the second term is due to what is often called anisotropic exchange [4] as well as dipole–dipole coupling.[1-3] For transition metal ions, and in particular, copper(II), anisotropic exchange is small except when J is large.[3,5]

When $|J| \gg \mathscr{J}_{ij}$ and the Zeeman and hyperfine interactions of the two ions, the energy levels consist of a singlet and triplet separated in energy by J. As defined in equation (1), $J > 0$ implies that the triplet is lowest in energy (ferromagnetic coupling) while $J < 0$ results in a singlet ground state (antiferromagnetic coupling). Antiferromagnetic coupling is certainly the most commonly occurring situation when J can be measured by means of conventional susceptibility techniques.[6] Recently, however, Hatfield *et al.* have reported triplet ground states in a number of cases, *e.g.* copper(II) diethyldithiocarbamate powders where they find $J = +24$ cm^{-1}.[7] This and other similar examples will be discussed further on the basis of our e.s.r. measurements.

In the case of copper acetate, Bleaney and Bowers [5] proposed a model for anisotropic exchange which led to a connection between the axial zero field splitting parameter, for the triplet state, D, and J. Their result gave only order of magnitude agreement with experiment, as did the subsequent refinements of it.[8] For $|J| \lesssim 30$ cm^{-1} the dominant contribution to $\mathscr{J}$ will come about from dipolar coupling. We cannot be sure in general what the upper limit of J for this result to hold will be, but our results for the copper(II) pyridine *N*-oxide complex provide some sort of clue as will be discussed later. From this point it will be assumed that for our present considerations, $\mathscr{J}$ is entirely due to the dipole interaction.

The Dipole–Dipole Interaction.—Let $\boldsymbol{\mu}_1$ and $\boldsymbol{\mu}_2$ be the magnetic dipole moments of the ions 1 and 2 respectively. If r is the copper(II)–copper(II) internuclear separation then the dipole–dipole interaction between the two ions is

$$\mathscr{H}_{\text{dip}} = \frac{\boldsymbol{\mu}_1 \cdot \boldsymbol{\mu}_2}{r^3} - \frac{3(\boldsymbol{\mu}_1 \cdot \mathbf{r})(\boldsymbol{\mu}_2 \cdot \mathbf{r})}{r^5} \qquad (2)$$

[4] P. Erdos, *J. Phys. Chem. Solids*, 1966, **27**, 1705.
[5] B. Bleaney and K. D. Bowers, *Proc. Roy. Soc.*, 1952, *A*, **214**, 451.
[6] M. Kato, H. B. Jonassen, and J. C. Fanning, *Chem. Rev.*, 1964, **64**, 99.
[7] J. F. Villa and W. E. Hatfield, *Inorg. Chim. Acta*, 1971, **5**, 145, and *Inorg. Chem.*, 1971, **10**, 2038; (Villa and Hatfield use $2J$ where we use J).
[8] I. G. Ross, *Trans. Faraday Soc.*, 1959, **55**, 1057 and I. G. Ross and J. Yates, *Trans. Faraday Soc.*, 1959, **55**, 1064.

For ions which possess orbital as well as spin angular momentum, there may be additional terms required in equation (2). As pointed out recently by Abragam and Bleaney,[9] the general interaction between such ions can always be considered in terms of a multipole expansion of which equation (2) is the first term. $\mathscr{H}_{dip}$ depends on r^{-3} as well as on angular factors. The next highest term in the expansion will be of order r^{-5} and we will neglect it here. Such a term may sometimes be important for the rare earths.[10]

The point dipole approach may conceivably break down when there is significant overlap of the electron distributions of the two ions ($r < 3$ Å) or when there is considerable delocalisation of the unpaired electron density onto the ligands. Whether we are always justified in identifying the r in equation (2), extracted from the e.s.r. data, with the true internuclear separation between the copper(II) ions can best be judged from our results.

$\mathscr{H}_{dip}$ must now be put in a form which will allow us to work out the energy matrix for the dimer. The magnetic moments $\boldsymbol{\mu}_1$ and $\boldsymbol{\mu}_2$ may be represented in terms of the effective spins of the ions as

$$\boldsymbol{\mu}_i = \beta \sum_{\alpha = x,y,z} g_{i\alpha} S_{i\alpha} \boldsymbol{\alpha}; \quad i = 1, 2 \qquad (3)$$

x, y, and z are the principal axes of the g tensor and the $\boldsymbol{\alpha}$ the unit vectors along these axes. Then the dipolar interaction becomes

$$\mathscr{H}_{dip} = \sum_{\alpha,\gamma = x,y,z} \mathscr{J}_{\alpha\gamma} S_{1\gamma} S_{2\gamma} \qquad (4)$$

where

$$\mathscr{J}_{\alpha\gamma} = \frac{\beta^2}{r^3} \left\{ g_{1\alpha} \sum_{\xi = x,y,z} g_{2\xi} \left(1 - 3 \sum_{\xi = x,y,z} \sigma_\xi \sigma_\alpha \right) \right\} \qquad (5)$$

The σ_α are the direction cosines of r with respect to the x, y, and z axes. Since the two ions are assumed identical, $g_1 \equiv g_2$ so we put $g_{1x} = g_{2x} = g_x$, *etc.* Using equation (5) we may thus write for the triclinic case (Table 1) putting $\beta_r = \beta^2/r^3$.

$$\begin{aligned}
\mathscr{J}_{xx} &= g_x^2(1 - 3 \sin^2 \eta \sin^2 \xi)\beta_r \\
\mathscr{J}_{yy} &= g_y^2(1 - 3 \cos^2 \eta \sin^2 \xi)\beta_r \\
\mathscr{J}_{zz} &= g_z^2(1 - 3 \cos^2 \xi)\beta_r \\
\mathscr{J}_{xy} &= \mathscr{J}_{yx} = -3 g_x g_y \sin^2 \xi \sin \eta \cos \eta \, \beta_r \\
\mathscr{J}_{xz} &= \mathscr{J}_{zx} = -3 g_z g_x \sin \xi \cos \xi \sin \eta \, \beta_r \\
\mathscr{J}_{yz} &= \mathscr{J}_{zy} = -3 g_z g_y \sin \xi \cos \xi \cos \eta \, \beta_r
\end{aligned} \qquad (6)$$

The Spin Hamiltonian in a Magnetic Field.—It is assumed that the spin Hamiltonian for ion $i (i = 1, 2)$ is

$$\mathscr{H}_i = \sum_{j = x,y,z} (\beta g_j S_{ij} H_j + A_j S_{ij} I_{ij})$$

where H_j, A_j, and I_{ij} are the j components of the applied field, the hyperfine interaction and the i ion nuclear spin respectively. Then the total spin Hamiltonian for the pair may be written

$$\mathscr{H} = \mathscr{H}_1 + \mathscr{H}_2 + \mathscr{H}_{int} \qquad (7)$$

In this paper we will discuss the perturbation theory solutions to equation (7) subject to the restrictions $\mathscr{H}_i(\text{Zeeman}) \gg \mathscr{H}_{dip}$ and $|J| \lesssim 30$ cm^{-1}. We shall see that where $|J| \ll h\nu$, the microwave energy, we must consider all possible states. When $|J| \gg h\nu$ we may treat the e.s.r. as arising simply within the triplet state, the singlet state being removed in energy an amount J from the triplet. It appears from our computer results, taking $|J| \gtrsim 3h\nu$ ensures that the states have true singlet–triplet character.

A complication arises when $|J| \simeq h\nu$ for then one of the zero order energy denominators in the perturbation

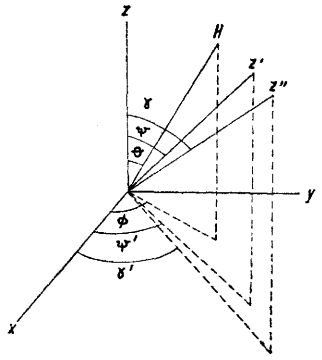

FIGURE 2 Orientation of magnetic field, and electron and nuclear quantisation axes (z' and z''). See Appendix for relationships between angles

theory vanishes. A first attempt to deal with this situation is discussed in the Appendix. Preliminary computer simulated spectra for this case appear to be quite different from those obtained when $|J|$ is either small or large with respect to $h\nu$. This point is not pursued further since the examples presented later fall into the category $|J| \gg h\nu$, except in one case where J is not known for certain.

In the strong field limit, and for an arbitrary orientation of the magnetic field, the Zeeman and hyperfine interactions are transformed into a representation in which the Zeeman interaction is diagonal (Zeeman representation). The electron and nuclear quantisation directions are z' and z'' respectively and are shown in Figure 2.

$$\begin{aligned}
\mathscr{H}_1 + \mathscr{H}_2 = \sum_{i = 1,2} (&g\beta H S_{iz'} + K S_{iz'} I_{iz''} + \tau_1 S_{ix'} I_{ix''} + \\
&\tau_2 S_{iy'} I_{iy''} + \tau_3 S_{iy'} I_{ix''} + \tau_4 S_{ix'} I_{iz''} + \tau_5 S_{iy'} I_{iz''})
\end{aligned} \qquad (8)$$

where

$$\begin{aligned}
g^2 &= g_z^2 \cos^2 \theta + g_\perp^2 \sin^2 \theta; \\
g_\perp^2 &= g_x^2 \cos^2 \phi + g_y^2 \sin^2 \phi \\
K^2 g^2 &= A_z^2 g_z^2 \cos^2 \theta + A_\perp^2 g_\perp^2 \sin^2 \theta; \\
g_\perp^2 A_\perp^2 &= A_x^2 g_x^2 \cos^2 \phi + A_y^2 g_y^2 \sin^2 \phi
\end{aligned} \qquad (9)$$

and τ_1—τ_5 are defined in the Appendix.[11]

[9] A. Abragam and B. Bleaney, 'Electron Paramagnetic Resonance of Transition Ions,' Oxford, 1970.

[10] J. M. Baker, *Reports Progr. Phys.*, 1971, **34**, 109.

[11] A. D. Toy, S. H. H. Chaston, J. R. Pilbrow, and T. D. Smith, *Inorg. Chem.*, 1971, **10**, 2219.

Transformation of $\mathcal{H}_{int}$.—It can easily be shown that $\mathcal{H}_{int}$ may be written in the Zeeman representation.

$$\mathcal{H}_{int} = -J\mathbf{S}_{1'} \cdot \mathbf{S}_{2'} + \sum_{p',q' = x,y,z} D_{p'q'} S_{1p'} S_{2q'} \quad (10)$$

where

$$D_{p'q'} = \sum_{r,s = x,y,z} l_{rp'} l_{sq'} \mathcal{J}_{rs} \quad (11)$$

and

$$(l_{rp'}) = \begin{bmatrix} \cos\psi\cos\psi' & -\sin\psi' & \sin\psi\cos\psi' \\ \cos\psi\sin\psi' & \cos\psi' & \sin\psi\sin\psi' \\ -\sin\psi & 0 & \cos\psi \end{bmatrix} \quad (12)$$

The polar angles ψ,ψ' are defined in Figure 2, and the relations between them and θ and ϕ given in the Appendix.

Perturbation Theory in the Zeeman Representation.—To develop the necessary perturbation theory we describe the states as simple product functions in an uncoupled representation using the notation

$$|\pm\pm m_1 m_2\rangle \equiv |M_1 = \pm\tfrac{1}{2}, M_2 = \pm\tfrac{1}{2}, m_1 m_2\rangle \equiv |M_1\rangle|m_1\rangle|M_2\rangle|m_2\rangle \quad (13)$$

M_i and m_i are the effective spin and nuclear quantum numbers for ion i. Since $S_i = \frac{1}{2}$, $M_i = \pm\frac{1}{2}$ so we simply use $\pm$ in equation (13).

The energy matrix, excluding the terms in τ_1, τ_2, and τ_3, is given in the Appendix (equation A4). We note in passing that some of the quantities in (A5) correspond to D_1, D_2, and D_3 used in our previous work concerning axial dimers.[1,2,10,11] Thus

$$D_1 = \tfrac{1}{4}D_{zz},\ D_2 = \tfrac{1}{4}(D_{xx} + D_{yy}),\ D_3 = \tfrac{1}{4}(D_{xx} - D_{yy}),\ D_2' = D_2 - \tfrac{1}{2}J \quad (14)$$

Let us define $D_6 = (D_{yx} - D_{xy})/4$.

Inspection of equation (A4) will show that apart from the terms in K, the diagonal energies for the $|+\ -m_1 m_2\rangle$ and $|-\ +m_1 m_2\rangle$ states are equal. Therefore we must diagonalise the inner 2×2 part of that energy matrix before proceeding with the use of perturbation theory. This matrix has energy eigenvalues and eigenfunctions

$$E_2 = -\frac{D'_{zz}}{4} + \Phi,\ |\psi_2\rangle = (U + iV)|+\ -m_1 m_2\rangle + b|-\ +m_1 m_2\rangle \quad (15)$$

$$E_4 = -\frac{D'_{zz}}{4} - \Phi,\ |\psi_4\rangle = (W + iX)|+\ -m_1 m_2\rangle + d\,|-\ +m_1 m_2\rangle$$

where $D'_{zz'} = D_{zz} - J$ and Φ, U, V, W, X, b, and d are all defined in the Appendix. If we write $|\psi_1\rangle \equiv |++m_1 m_2\rangle$ and $|\psi_3\rangle \equiv |--m_2 m_2\rangle$ then $|\psi_1\rangle$—$|\psi_4\rangle$ is the new basis set to describe the problem.

Following the inner 2×2 diagonalisation procedure the energy matrix takes the form given in equation (A6) of the Appendix. The energies, E_1—E_4, correct to second order in $\mathcal{H}_{dip}$ and the wavefunctions to first order are given in equations (A10) and (A11) and are easily obtained from equation (A6). From these energy levels we calculate transition positions for the four $\Delta M = 1$ transitions and the single $\Delta M = 2$ transition for each pair of values of m_1 and m_2. Transition intensities may be obtained from the wavefunctions. Expressions for resonance field positions and intensities are given later in this section.

In the wavefunctions given in equation (15) we include the imaginary parts with coefficients V and X. Both V and X are zero for the model assumed since we have taken the dimer to possess inversion symmetry. We retain V and X for these subsequent expressions will all apply to a more general situation; all that will need to be changed are the expressions for $\mathcal{J}_{\alpha\gamma}$.

The Effect of the Size of J.—(i) $|J| \ll h\nu$. The states $|\psi_1\rangle$, $|\psi_2\rangle$, and $|\psi_3\rangle$ do not constitute a 'pure' triplet, nor is $|\psi_4\rangle$ a 'pure' singlet. Therefore all four states must be retained in the calculations. As mentioned earlier there are $(2I_1 + 1)(2I_2 + 1)$ such 'singlets' and 'triplets' corresponding to every pair of allowed m_1 and m_2 values. And so when nuclear hyperfine terms are included, there are not 4 $\Delta M = 1$ transitions but 64 for copper(II) pairs, and 16 $\Delta M = 2$ transitions. In the case of $\Delta M = 2$ transitions, the transition probabilities will have their maximum value away from the internuclear axis.[3]

(ii) $h\nu \ll |J| \lesssim 30$ cm^{-1}. Here J is restricted to values sufficiently small that pseudo-dipolar corrections are not required in the D_{pq}, but sufficiently large that the four states split into a triplet and a singlet, separated in energy an amount J. Retention of J in the calculations automatically ensures that $U \longrightarrow \pm b = 2^{-\frac{1}{2}}$ and $V \longrightarrow \mp d = 2^{-\frac{1}{2}}$ where the upper sign refers to $J < 0$ and the lower sign to $J > 0$.

In such a case, the e.s.r. is due to the triplet state alone. We may therefore simplify the calculations by eliminating those terms which depend on the singlet state and for copper(II) pairs we find there are but 32 $\Delta M = 1$ transitions. We could of course treat the e.s.r. as arising from a state with $S = 1$, and describe the ground state splitting within the triplet by means of the usual D and E terms in a spin Hamiltonian. This approach was used by Bleaney and Bowers,[5] Villa and Hatfield,[7] Belford and Chasteen,[12] Cowsik *et al.*,[13] and Buluggiu *et al.*[14] For these low symmetry cases considered here, we note that the fine structure tensor, represented by D and E, will have one principal axis close to the internuclear axis but not exactly along it because of g anisotropy. We have worked out general expressions relating D and E to the D_{pq} but they do not assist in making our treatment any more tractable. When one considers the hyperfine inter-

[12] (*a*) N. D. Chasteen and R. L. Belford, *Inorg. Chem.*, 1970, **9**, 169 and (*b*) *errata ibid.*, 1970, **9**, 2805.

[13] R. K. Cowsik, G. Rangarajan, and R. Srinivasan, *Chem. Phys. Letters*, 1971, **8**, 136.

[14] E. Buluggiu, G. Da Scola, D. C. Giori, and V. Varacca, *Phys. Stat. Sol.* (b), 1971, **45**, 217.

action one must use the individual ion electronic effective spins in evaluating the matrix elements. Our approach using the dipolar tensor in terms of the D_{pq} is, therefore, much easier to handle overall.

Transition Fields and Intensities (All variables defined in text or Appendix).—$\Delta M = 1$.

$$\begin{aligned}
1 \longrightarrow 2\ H_1 &= H_0 + H_0\{-D_{zz}'/2 - K(m_1 + m_2)/2 + \\
&\quad \Phi - [2V_{12} + \tfrac{1}{2}V_{34} + V_{78} - V_{56}]\}/W_0 \\
2 \longrightarrow 2\ H_2 &= H_0 + H_0\{D_{zz}'/2 - K(m_1 + m_2)/2 - \\
&\quad \Phi - [-V_{12} + \tfrac{1}{2}V_{34} + 2V_{56} + V_{9,10}]\}/W_0 \\
1 \longrightarrow 4\ H_3 &= H_0 + H_0\{-D_{zz}'/2 - K(m_1 + m_2)/2 - \\
&\quad \Phi - [V_{12} + \tfrac{1}{2}V_{34} + 2V_{78} - V_{9,10}]\}/W_0 \\
4 \longrightarrow 3\ H_4 &= H_0 + H_0\{D_{zz}'/2 - K(m_1 + m_2)/2 + \\
&\quad \Phi - [-V_{78} + 2V_{9,10} + \tfrac{1}{2}V_{34} + V_{56}]\}/W_0
\end{aligned} \tag{16}$$

where

$V_{ij} = (S_i^2 + S_j^2)/W_0$ [*N.B.* $V_{9,10} = (S_9^2 + S_{10}^2)/W_0$], $W_0 = h\nu$ and $H_0 = h\nu/g\beta$.

The corresponding transition intensities to first order are

$$P_{1,2} = \tfrac{1}{4}[(U + b)^2 + V^2](1 \pm S_3/W_0)$$
and
$$P_{3,4} = \tfrac{1}{4}[(W + d)^2 + X^2](1 \mp S_3/W_0) \tag{17}$$

There are, of course, second order terms which should be added in to equation (17). It turned out that such terms did not noticeably affect the computed spectra and so they were left out in the calculations.

$\Delta M = 2$ *Transitions.*—

$$\begin{aligned}
H(\Delta M = 2) = H_0/2 - H_0[K(m_1 + m_2)/2 + V_{12} + \\
V_{34} + V_{56} + V_{78} + V_{9,10}]/W_0
\end{aligned} \tag{18}$$

and to second order, there being no result to first order,

$$\begin{aligned}
P(\Delta M = 2) = \{&[(U + b)(S_1 - S_5) + V(S_2 + S_6) \\
&+ (W + d)(S_7 - S_9) + X(S_8 - S_{10})]^2 \\
&+ [(U + b)(S_2 - S_6) - V(S_1 + S_5) \\
&+ (W + d)\ (S_8 + S_{10}) - X(S_7 + S_9)]^2\}/W_0^2
\end{aligned} \tag{19}$$

Hyperfine Terms τ_1—τ_3.—These terms from equation (8) lead to additional second order energy corrections which are listed in the Appendix. They give rise to magnetic field corrections as follows:

$$\begin{aligned}
\Delta H_{1,2} &= -H_0\{I(I + 1) - m_{1,2}{}^2b^2 - m_{2,1}a^2\} \\
&\qquad (\tau_1^2 + \tau_2^2 + \tau_3^2)/4W_0^2 \\
\Delta H_{3,4} &= -H_0\{I(I + 1) - m_{1,2}{}^2a^2 - m_{2,1}{}^2b^2\} \\
&\qquad (\tau_1^2 + \tau_2^2 + \tau_3^2)/4W_0^2
\end{aligned} \tag{20}$$

$$\begin{aligned}
\text{and } \Delta H(\Delta M = 2) &= -H_0\{I(I + 1) - m_1^2 - m_2^2\} \\
&\qquad (\tau_1^2 + \tau_2^2 + \tau_3^2)/4W_0^2
\end{aligned}$$

where $a^2 = U^2 + V^2 = d^2$ and $c^2 = W^2 + X^2 = b^2$ (21)

Perturbation Denominators.—In obtaining equations (16)—(21) we note that for $\Delta M = 1$ transitions $\Delta_{13}{}^0 = 2g\beta H_0$ and the other $\Delta_{ij}{}^0 = g\beta H_0$, whereas for the $\Delta M = 2$ transitions, $\Delta_{13}{}^0 = g\beta H_0$ and the other $\Delta_{ij}{}^0 = \frac{1}{2}g\beta H_0$ since the latter transitions occur at about half the magnetic field of the former. $H_0 = h\nu/g\beta$ and is the field at which transitions will occur in the absence of dipolar and hyperfine interactions.

Modifications when $|J| \gg h\nu$.—It was noted earlier that when this condition holds, e.s.r. occurs within the 'triplets' which are some distance in energy away from the 'singlets'. We note the following modifications with respect to equations (16), (18), and (19): $J < 0$. The triplet levels are $|\psi_1\rangle$, $|\psi_2\rangle$, and $|\psi_3\rangle$. Calculation of the e.s.r. spectrum requires the use of only H_1, H_2, and $H(\Delta M = 2)$. The following parameters may be set equal to zero: $S_7 = S_8 = S_9 = S_{10} = V_{78} = V_{9,10} \equiv 0$. $J > 0$ $|\psi_1\rangle$, $|\psi_4\rangle$, and $|\psi_3\rangle$ are now the triplet levels. Therefore only H_3, H_4 are needed as well as $H(\Delta M = 2)$ and we may put $S_1 = S_2 = S_5 = S_6 = V_{12} = V_{56} \equiv 0$.

SIMULATION OF E.S.R. SPECTRA

In frozen solutions or powder samples, it is assumed that all orientations of the metal ion pair complexes with respect to the applied magnetic field are possible. Thus a general expression for the e.s.r. lineshape may be written,

$$f(H) = \sum_{n=1}^{N} \int_{\phi=0}^{\Phi'} \int_{\theta=0}^{\Theta'} P(n,\theta,\phi)G(H,n,\theta,\phi)d\cos\theta \tag{25}$$

where N = the number of transitions, Φ' and Θ' the upper values of the polar angles θ and ϕ. $P(n,\theta,\phi)$ is the transition probability of the nth transition for a complex for which H makes polar angles θ and ϕ with respect to the x, y, and z axes as defined in Figure 1. $P(n,\theta,\phi)$ consists of the two factors, the P_i of equations (17) or $P(\Delta M = 2)$, equation (19), and a term representing the effect of g-anisotropy.[15]

Gaussian lineshapes were used throughout. Since we wished to calculate first derivative spectra, the appropriate form for a normalised Gaussian first derivative lineshape at a particular magnetic field H is

$$\begin{aligned}
G(H,n,\theta,\phi) = -\{&[H - H(n,\theta,\phi)]/\sigma^3\} \\
&\exp\{[H - H(n,\theta,\phi)]^2/2\sigma^2\}
\end{aligned} \tag{26}$$

where $H(n,\theta,\phi)$ is the transition position of the nth transition of a dimer complex for which H makes polar angles θ and ϕ with the x, y, and z axes. $H(n,\theta,\phi)$ is one of H_1—H_4 or $H(\Delta M = 2)$ in equation (16) or (18) respectively. σ Is the Gaussian half-width.

Evaluation of the integrals in equation (25) is not possible using analytic methods, and so we must approximate equation (25) in some way. The simplest approximation is the trapezoidal rule whereby we replace the integrals by summations over finite intervals. Therefore

$$f(H) \simeq \sum_{n=1}^{N} \sum_{\phi=0}^{\Phi'} \sum_{\theta=0}^{\Theta'} P(n,\theta,\phi)G(H,n,\theta,\phi)\Delta\cos\theta,\ \Delta\phi \tag{27}$$

[15] J. R. Pilbrow, *Mol. Phys.*, 1969, **16**, 307.

To ensure smoothness in the final result, $f(H)$ plotted against H, one must find, by trial and error, a sufficient number of orientations of θ and ϕ which avoids computer noise. For θ in the range $\theta \longrightarrow 90°$ equal intervals of θ were used up to 43·6° followed by equal intervals of $\Delta \cos \theta$. This precaution avoids problems caused at $\theta \sim 90°$ where $\cos \theta$ is changing rapidly and allows one to work with slightly larger intervals. For ϕ, equal increments were used.

Equation (21) was evaluated using a FORTRAN program on the CDC 3200 computer at the Monash University Computer Centre. The program evaluates the analytical results for $H(n,\theta,\phi)$ and $P(n,\theta,\phi)$ for a orientation (θ,ϕ) and sums the contributions to $f(H)$ at specified output values of H. In the case of Gaussian lines, to save computer time, a contribution from a given transition is cut off at $\pm 3\sigma$. The final curve is an array of points $[f(H),H]$ printed by the computer line printer as well as a continuous curve on some convenient scale drawn by an off-line CALLCOMP graph plotter.

For the monoclinic symmetry case (Table 1), appropriate to the examples presented in this paper, we require $\Theta' = 180°$ and $\Phi' = 90°$. Triclinic symmetry requires $\Phi' = 180°$ instead.

Estimation of Errors.—In no case can we claim an exact match between experimental and computer simulated curves in every detail of line position or lineshape. We have been unable to derive our results using a least squares fitting approach for this would have made computer running time prohibitive. We have relied on visual fitting of the results and have used an arbitrary criterion that $\Delta M = 2$ fits should match most peak positions to about ± 5 G and $\Delta M = 1$ peaks to better than ± 10 G wherever possible. Experimental peaks are measured to an accuracy of ± 5 G. Variations of the results outside these ranges by means of adjustment of the spin Hamiltonian and structural parameters give an indication of what we may regard as errors in our final results. This approach does not represent a statistical best fit analysis, nor should our results be regarded in that way.

There is one slight difficulty in presenting the experimental results and theoretical curves produced by the CALLCOMP graph plotter on the same diagram. The magnetic field sweep of our spectrometer is not quite linear throughout the entire field range 1200—4000 G and, therefore, the field sweep assumed for the CALLCOMP plots is an average value for the particular field range required. However our fits are primarily judged on how well the various peaks match, not on how well a particular CALLCOMP spectrum overlays the experimental one.

In addition, some of the experimental results show a certain amount of baseline drift as well as superposition of residual copper(II) monomer spectra. No correction has been made for these effects, and so in judging the goodness of fit from our results it is best to be guided by overall peak positions.

From a study of our results, it is clear that the spectra are most sensitive to the values of r, ξ, g_z, A_z, g_x, and g_y. In no case were we able to determine values of A_x or A_y with any certainty.

In some cases better results were obtained with an anisotropic linewidth, but we do not claim to have determined the linewidths to high precision in any case. Linewidth anisotropy is included by means of the equation

$$\sigma = \{(g_x^2 W_x^2 \cos^2 \phi + g_y^2 W_y^2 \sin^2 \phi) \sin^2 \theta + g_z^2 W_z^2 \cos^2 \theta\}^{\frac{1}{2}}/g \quad (28)$$

W_x, W_y, and W_z are the principal linewidth component assumed to be parallel to the x, y, and z axes (Figure 1).

Our analysis is based on the use of perturbation theory to second order in $\mathcal{H}_{\text{dip}}$ and the hyperfine terms. It will be seen in our results that some small discrepancies do occur when comparison of results for $\Delta M = 1$ and $\Delta M = 2$ spectra is made in a given case. This is thought to have its origin in the fact that second order corrections while good for the $\Delta M = 2$ spectra and for the high field end of the $\Delta M = 1$ spectrum are likely to be less good at the low field end of the $\Delta M = 1$ spectrum. For this reason it has proved difficult to match simultaneously both high field and low field $\Delta M = 1$ peaks as well as the $\Delta M = 2$ spectra to the previously mentioned tolerances. Therefore particularly the g-values are less precisely known than if a computer diagonalisation procedure were practicable.

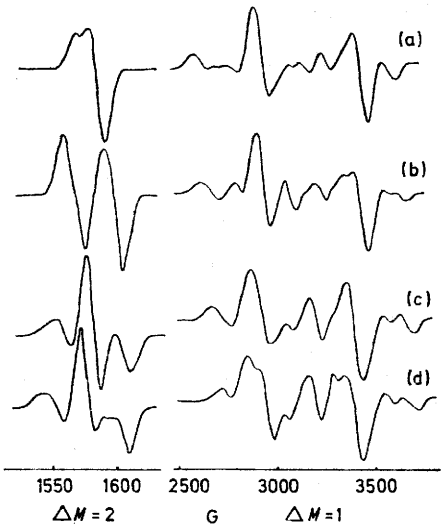

FIGURE 3 Theoretical e.s.r. spectra due to monoclinic dimer as ξ is varied. (a) $\xi = 0°$ (orthorhombic), (b) $\xi = 30°$, (c) $\xi = 60°$, (d) $\xi = 90°$ (orthorhombic). Other parameters are $r = 3{\cdot}8$ Å, $g_x = 2{\cdot}02$, $g_y = 2{\cdot}015$, $g_z = 2{\cdot}08$, $A_z = A_y = A_x = 0$, $W_x = W_y = W_z = 30$ G ($\Delta M = 1$), 5 G ($\Delta M = 2$), $J = -20$ cm^{-1}, microwave frequency 9081 MHz

However neither r nor ξ are noticeably affected by this problem.

The Effect of Low Symmetry.—To illustrate the effects of low symmetry on calculated spectra, we first consider some results in the absence of hyperfine interactions. For the monoclinic case, the variation in the spectrum

as ξ is varied from 0 to 90° is shown in Figure 3. In these and the later results 90 orientations of θ and eight orientations of ϕ proved generally quite satisfactory and were sufficient to avoid computer noise in the output. At both $\xi = 0$ and 90° the symmetry becomes

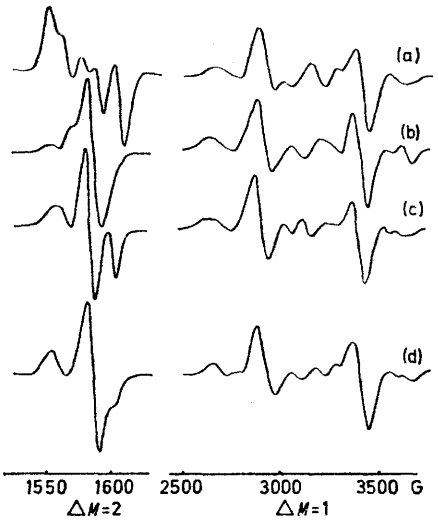

FIGURE 4 Theoretical e.s.r. spectra due to triclinic dimer as η is varied and $\xi = 45°$ (a) $\eta = 0°$ (monoclinic), (b) $\eta = 15°$, (c) $\eta = 30°$, (d) $\eta = 45°$. Other parameters are $r = 3{\cdot}8$ Å, $g_x = 2{\cdot}02$, $g_y = 2{\cdot}015$, $g_z = 2{\cdot}08$, $A_x = A_y = A_z = 0$, $W_x = W_y = W_z = 30$ G ($\Delta M = 1$), 5 G ($\Delta M = 2$), $J = -20$ cm^{-1}, microwave frequency 9081 MHz

orthorhombic. Triclinic and monoclinic cases are distinguishable only when $g_x \neq g_y$ and/or $A_x \neq A_y$. Figure 4 shows the variation in the triclinic case as η runs from 0 to 45°. For η in the range 45—90°, the same result may be repeated by interchanging x and y axes. The axial limit, the subject of earlier work,[1,2] occurs when $g_x = g_y$, $A_x = A_y$ and $\xi = 0$.

The effect of the hyperfine interaction is as follows. In the limit in which the triplet lies well away from the singlet, the 16-line hyperfine structure, in the case of copper(II) dimers, present on each $\Delta M = 1$ and $\Delta M = 2$ transition simplifies to a seven-line pattern with intensities 1 : 2 : 3 : 4 : 3 : 2 : 1 and a line spacing one-half that of the spectrum due to one of the copper(II) ions on its own. When the coupling is weak, the hyperfine pattern, while it may approximate to a seven-line pattern, will generally be more complicated.

Identification of the Spectra.—In the $\Delta M = 1$ spectrum, characteristically there are two very strong peaks spaced about 600 G on either side of g *ca.* 2 when r *ca.* 3·5 Å. On the low field side of the lower of these peaks, frequently there is a resolved seven-line group, intensities 1 : 2 : 3 : 4 : 3 : 2 : 1, while further structure is often found about the strong high field peak.

In the axial limit, the resolved structure, including the seven-line group arises from those molecules for which H is alone the z axis ('z' lines). The strong lines, with generally no hyperfine structure, arise from those molecules for which H is aligned in the xy plane ('x' or 'y' lines) where the lack of hyperfine structure is a result of the smaller hyperfine component in the xy plane compared with that along the z-axis.

In the monoclinic case, where the copper(II)–copper(II) internuclear axis makes an angle ξ with z, the aforementioned seven-line pattern will arise basically from those molecules for which H is close to the internuclear axis ('r' lines). The strong pair of lines will arise most probably from those molecules for which H is parallel to the x-axis. There may be structure in certain cases from molecules for which H is at an angle close to $\xi + 90°$ from z, the remaining dipolar principal direction. It is quite possible that there are other orientations of the molecules, different from the g or dipolar principal directions where the transitions minimise or maximise with respect to H, and which should give rise to additional peaks in the spectrum.

We have calculated spectra appropriate to single crystals of copper(II) diethyldithiocarbamate, using the value from our later computer fits, in the xz, yz, and xy planes and have verified the conclusions of the previous paragraphs.

In Figure 5 there is a simplified schematic representation of the energy levels indicating how the main peaks in the spectra of copper(II) dimers arise. The effect of the size of J is indicated.

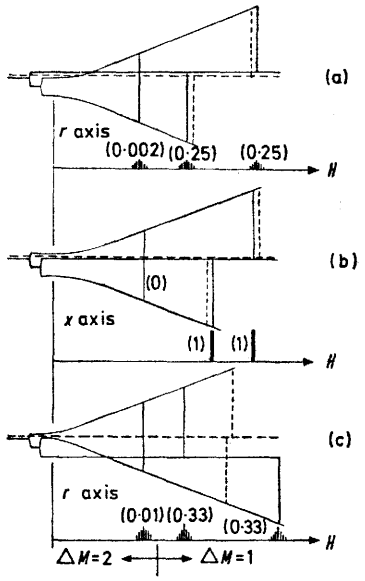

FIGURE 5 Schematic energy level diagrams showing origin of peaks in powder (or frozen solution) dimer spectra when $J = 0$ (not to scale). – – – – Indicates 'singlet' level. (a) H along r axis, (b) H along x axis, (c) H in zy plane normal to r axis ($r\perp$). $\Delta M = 1$ and 2 Transitions within triplet shown by |. Hyperfine structure is depicted underneath each energy level diagram. ¦ Indicates 'singlet'–'triplet' transitions weakly allowed when $J \ll h\nu$. When $J \neq 0$, 'singlet' moves away from 'triplet' and the additional lines cannot occur at normal fields. Numbers in parentheses are relative intensities. Resulting spectral intensities in powder modified by angular distribution of dimers.

E.S.R. RESULTS AND STRUCTURAL CONSIDERATIONS

Th ability of copper(II) when part of an essentially planar chelate structure to achieve five-co-ordination

by bonding to an atom of a neighbouring centrosymmetric molecule, thereby forming a dimeric unit, is of common occurrence. The symmetry of the pair system thus formed under these circumstances is closely similar to that shown by Figure 1 with $\eta = 0$, the monoclinic case defined in Table 1. It is this situation which is covered by the theoretical discussion in this paper.

An important aspect of this study is the relationship of the parameters r and ξ to similar quantities determined from X-ray crystallographic information on the dimeric complex. In the examples studied here, e.s.r. and X-ray data are found to be compatible for copper diethyldithiocarbamate in the zinc host and copper complexes with pyridine N-oxide and salicylaldehyde. For copper(II) tartrate we discuss reasons why the data are not entirely compatible.

It must be emphasised that the approach *via* e.s.r. is not the same as that involved in X-ray structure determination. Especially is this true in those examples where the e.s.r. data is obtained from frozen solutions of the dimer in some suitable solvent. In all cases, we use whatever structural data already exists for the solid compound, as well as any e.s.r. parameters for powders, single crystals, or solutions of the same or similar system to provide suitable starting values for our computer simulations.

In those cases where we observe both $\Delta M = 2$ and sufficient lines from the $\Delta M = 1$ spectrum of the dimer, we usually attempt the simulation of the $\Delta M = 2$ spectrum first so as to save computer time. The quantities ξ, r, and spin Hamiltonian parameters thus determined are then used to simulate the $\Delta M = 1$ lines. Subsequent refinements involve computation of both kinds of spectra, aimed at converging on a best-fit set of the parameters.

Copper(II) *Diethyldithiocarbamate.*—The molecular structure of crystalline copper(II) diethyldithiocarbamate may be described as a bimolecular unit in which each pair of centrosymmetrically related copper(II) ions, at the rather short distance of 3·59 Å, share sulphur atoms,[16] as shown by structure (I). The geometry

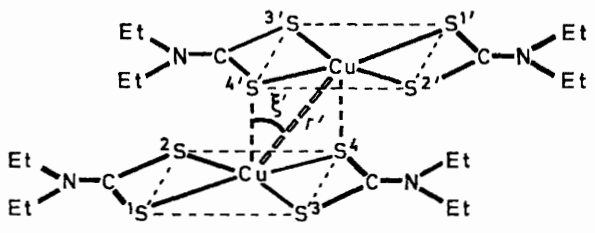

(I)

of the co-ordination of copper(II) here is closely related to a tetragonal pyramid with copper(II) having a co-ordination number of five with normal bonds to four sulphur atoms and a longer bond to a sulphur atom of the centrosymmetrically related molecule.

On the other hand in zinc(II) diethyldithiocarbamate

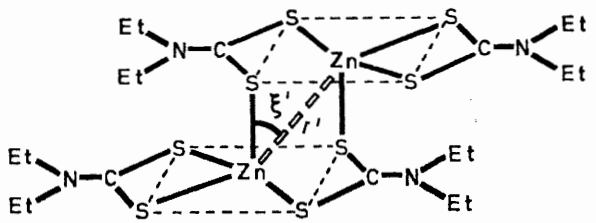

(II)

[structure (II)] each pair of centrosymmetrically related zinc atoms share sulphur atoms to form dimeric units in which each zinc atom is co-ordinated with five sulphur atoms in a distorted trigonal bipyramidal environment[17] ($r' = 3{\cdot}5$ Å). In addition the ligand molecule behaves in two ways in the same complex; one ligand forms a four-membered chelate ring and a second co-ordinates with two different zinc(II) ions while at the same time completing a chelate ring with a long approach distance. The four shortest bonds formed by any zinc(II) ion are directed at the corners of a distorted tetrahedron with the ligand molecules planar. In the dimeric unit formed by zinc(II) dimethyldithiocarbamate the zinc(II)–zinc(II) distance is 3·9 Å.[18] The dimethyldithiocarbamate groups deviate slightly from planarity and again two types of linking are discerned. One group is chelated directly to its own zinc(II) ion tetrahedron while two of the second type act as bridging ligands between the two zinc(II) tetrahedra. Thus the structural form of the dimeric zinc(II) diethyldithiocarbamate is sufficiently different from that of the copper(II) complex to raise the following question. When copper(II) diethyldithiocarbamate is incorporated into the host lattice of zinc(II) diethyldithiocarbamate, will the structural parameters of the dimeric copper(II) complex be similar to those observed in the pure copper(II) complex or will they lie closer to those of the dimeric units which act as the host lattice? It is the purpose of the present investigation to resolve this question using information derived from the e.s.r. spectra due to the dimeric copper(II) diethyldithiocarbamates formed under diamagnetic dilution conditions.

The e.s.r. spectra of copper(II) dialkyldithiocarbamates in frozen solution of chloroform containing small amounts of other solvents provide evidence for the existence of a dimeric form of the copper(II) complex under these conditions.[19] More recently it has been shown that the e.s.r. spectra of powder samples consisting of zinc diethyldithiocarbamate containing small amounts of copper(II) diethyldithiocarbamate are consistent with the view that again the copper(II) complex gives rise to dimeric species.[7,13] It is of interest to investigate the effects of the molecules comprising the

[16] M. Bonamico, G. Dessy, A. Mugnoli, A. Vaciago, and L. Zambonelli, *Acta Cryst.*, 1965, **19**, 886.

[17] M. Bonamico, G. Massone, and L. Zambonelli, *Acta Cryst.*, 1965, **19**, 898.

[18] H. P. Klug, *Acta Cryst.*, 1966, **21**, 536.

[19] A. D. Toy, T. D. Smith, and J. R. Pilbrow, *J. Chem. Soc.* (*A*), 1969, 1029.

host lattice on the structure of the dimeric form of copper(II) diethyldithiocarbamate. Magnetic susceptibility studies by Hatfield *et al.*[7] showed that the ground state of the dimer is the 'triplet' with the 'singlet' 24 cm^{-1} higher in energy. That is $J = +24$ cm^{-1}. For our later computer simulation of the e.s.r. spectra we can assume the 'triplet' solution described earlier, $|J| \gg h\nu$.

A necessary condition that is sought to obtain triplet state e.s.r. spectra is that the paramagnetic ion pair systems are magnetically isolated from one another. This is achieved by dilution in a diamagnetic host lattice which could affect the structural relationship between the units comprising the dimer molecule. The change of host lattice could be of critical importance particularly in cases where the relationship between the molecules in the pure state is controlled by packing considerations. On the other hand, the ability to monitor structural changes of the dimer molecule if they occur in a variety of host lattices using easily obtained experimental data offers an advantage over *X*-ray crystallographic techniques. Provided that the change of environment brought about by diamagnetic dilution is not critical in deciding the structural alignment in the copper(II) complexes, a reasonable starting point in accounting for the e.s.r. line shape of the triplet state spectra is to consider that the copper(II) ions possess a symmetry arrangement in pairs close to the monoclinic case defined in Table 1 and Figure 1.

The relationship of the *g* tensor axes to the crystal axes in copper(II) diethyldithiocarbamate was established by Weeks and Fackler [20] who found that in circumstances of diamagnetic dilution of copper(II) diethyldithiocarbamate by the zinc complex there is coincidence of the direction of g_z and the *z* axis of the complex (*i.e.* the normal to the least squares plane through the four sulphur atoms) to within 2·5° between the two vectors. Of the two principal axes that lie in the plane of the sulphur atoms, the *y*-axis, as we have defined it lies along the S(1)–Cu–S(4) direction. This direction contains the pair of bonds that are elongated in the zinc complex, a result which implies that the symmetry of the copper(II) ion within the complex is little altered as a result of incorporation into the host lattice provided by the zinc complex.

Fackler and Weeks [20] also studied the e.s.r. of copper(II) in nickel(II) diethyldithiocarbamate. This time the in plane *g*-values lie between the Cu–S bonds in contrast to the results in the zinc host. *X*-Ray structural data for nickel(II) diethyldithiocarbamate shows that the nickel ions are not packed in dimer fashion.[21]

E.S.R. Results.—Zinc diethyldithiocarbamate doped with various concentrations of the copper(II) complex was prepared by the coprecipitation of the complexes by the addition of a freshly prepared aqueous solution of sodium diethyldithiocarbamate to an aqueous solution of the metal sulphates. The precipitate was washed with water and dried over phosphorus pentoxide. The copper(II) to zinc ratio was varied over the range 1 : 10 to 1 : 500.

The *X*-band e.s.r. spectrum of a powder sample is shown in Figure 6. The $\Delta M = 1$ spectrum was seen most clearly at room temperature whereas the $\Delta M = 2$ spectrum was only observed at 77 K. These results are in broad agreement with those of Villa and Hatfield.[7] An essentially similar spectrum was obtained from zinc(II) dimethyldithiocarbamate doped with copper(II) dimethyldithiocarbamate. The use of cadmium(II) diethyldithiocarbamate as the host lattice also gave the same spectrum when doped with the copper(II) complex.

In Figure 6(a) we note that there is a very well resolved $\Delta M = 2$ spectrum *ca.* 1500 G. The $\Delta M = 1$ spectra,

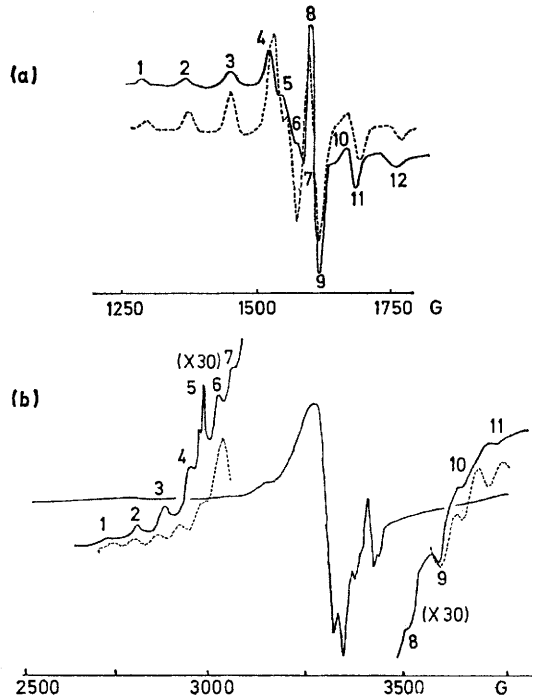

FIGURE 6 *X*-Band e.s.r. spectrum due to copper(II) in zinc(II)-diethyldithiocarbamate powder —— (a) $\Delta M = 2$ dimer spectrum, microwave frequency 9087 MHz, temperature 77 K, (b) $\Delta M = 1$ dimer spectrum and monomer spectrum, microwave frequency 9450 MHz, temperature 293 K. Computer simulated spectra – – – – obtained with parameters: $r = 3{\cdot}90 \pm 0{\cdot}05$ Å ($\Delta M = 2$) and $r = 3{\cdot}85 \pm 0{\cdot}05$ Å ($\Delta M = 1$), $\xi = 42 \pm 2°$, $g_x = 2{\cdot}020 \pm 0{\cdot}005$, $g_y = 2{\cdot}015 \pm 0{\cdot}005$, $g_z = 2{\cdot}070 \pm 0{\cdot}005$, $A_x = 0{\cdot}0027$, $A_y = 0{\cdot}0007$, $A_z = 0{\cdot}0148 \pm 0{\cdot}0003$ cm^{-1}, $W_x = W_y = W_z = 8$ G ($\Delta M = 2$) and 16 G ($\Delta M = 1$), $J = +24$ cm^{-1}. Errors in A_x and A_y not estimated. Simulated curves not on exactly same intensity scale as experimental

represented by a number of small peaks in the ranges 2700—3100 G and 3500—3750 G shown in Figure 6(b), are somewhat obscured by spectra from isolated copper(II) ions in the lattice.

Starting values of the spin Hamiltonian parameters for the computer simulated spectra were those reported

[20] M. J. Weeks and J. P. Fackler, *Inorg. Chem.*, 1968, **7**, 2548.
[21] M. Bonamico, G. Dessy, M. Mariani, A. Vaciago, and L. Zambonelli, *Acta Cryst.*, 1965, **19**, 619.

by Fackler and Weeks.[20] From the *X*-ray data we calculated $\xi' = 40°$ [22] in agreement with the value by Villa and Hatfield.[7]

In view of the overlap of $\Delta M = 1$ dimer spectra and the residual monomer spectrum, the $\Delta M = 2$ spectrum was simulated first and then the best-fit parameters thus determined were used to simulate the $\Delta M = 1$ spectrum. In Figure 6(b), peaks 1—4, 6, 8, 10, and 11 were associated with $\Delta M = 1$ 'r' lines. The sharp doublet (5) belongs to the monomer, as pointed out by Villa and Hatfield.[7] At 3590 G there is a somewhat stronger peak (9), which is believed to be the high field 'x' line. Computer simulated spectra are also shown in Figure 6. Overall, the $\Delta M = 2$ spectrum was fitted better than the $\Delta M = 1$ lines, partly because as we noted earlier, the second order perturbation corrections are probably least good for the low field $\Delta M = 1$ 'r' lines.

Upon proceeding with the simulation of the spectra, it was found to be necessary to reduce the g-values slightly from the values reported by Weeks and Fackler.[20]

The best-fit parameters accompany Figure 6 but values of ξ and r are given in Table 3. It can be seen that the value of $r = 3{\cdot}85 \pm 0{\cdot}05$ Å is larger than that of both the pure copper compound and the zinc host, but $\xi = \xi' = 40°$ in agreement with the copper case. Thus we conclude that in the zinc diethyldithiocarbamate, copper(II) ions are located as nearly as possible in a site commensurate with the pure copper compound, but with a larger copper(II)–copper(II) separation.

It was assumed that since Weeks and Fackler [20] had found three distinct g-values for copper(II) in zinc diethyldithiocarbamate that in the dimers there should still be orthorhombic symmetry. In addition although the value of A_z was subject to some adjustment, there was no good reason to alter the values of A_x and A_y taken from Weeks and Fackler's results especially since the simulated spectra were not particularly sensitive to variations in either of them. It was found that the overall agreement of the results worsened if axial g and A values were used.

E.s.r. experiments on copper-doped nickel(II) diethyldithiocarbamate gave no evidence of dimer spectra in agreement with the structure of the nickel compound discussed previously.

Bis(pyridine N*-oxide)copper*(II) *Nitrate.*—The crystal structure determination of bis(pyridine *N*-oxide)-copper(II) nitrate [23] has revealed that in the solid state it exists in a dimeric form where each five-co-ordinated copper(II) ion possesses a tetragonal pyramidal environment. From the structure, shown schematically in structure (III), it was deduced that $\xi' = 41°$ and $r' = 3{\cdot}46$ Å.[22]

Magnetic susceptibility studies indicate that the molecule has a magnetic moment of 1·90β per copper(II) ion.[24] The temperature dependence of the susceptibility gave a value of J *ca.* 30 cm^{-1}, which of course implies that the triplet is lowest in energy.

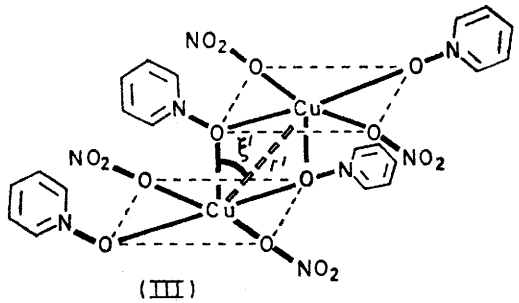

E.S.R. Results.—*X*-Band e.s.r. measurements were carried out at 77 K on bis(pyridine *N*-oxide)copper(II) nitrate doped into the corresponding zinc salt in a

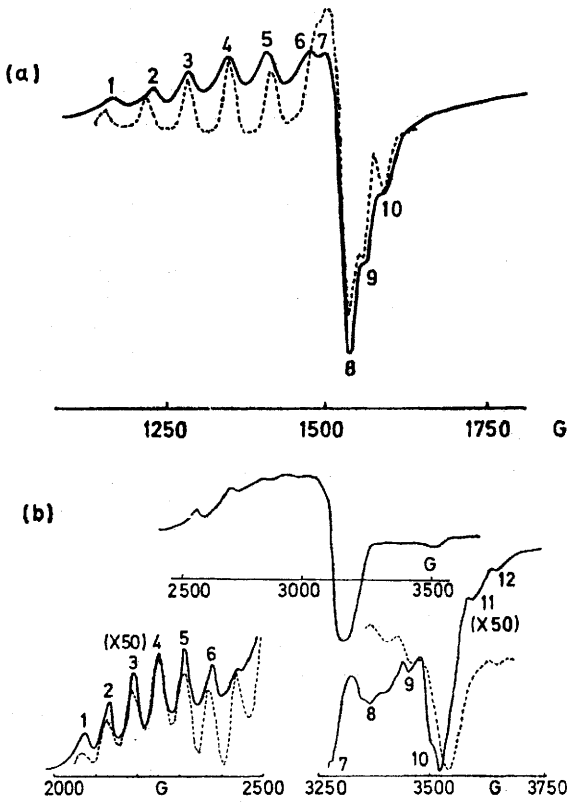

FIGURE 7 *X*-Band e.s.r. spectrum due to a powder sample of bis(pyridine *N*-oxide)copper(II)nitrate doped into the corresponding zinc salt in a 1 : 9 ratio. Microwave frequency 9140 MHz, temperature 77 K —— (a) $\Delta M = 2$ spectrum, (b) $\Delta M = 1$ spectrum and residual monomer spectrum. Computer simulated spectrum – – – – obtained with following parameters: $r = 3{\cdot}46 \pm 0{\cdot}05$ Å, $\xi = 41 \pm 1°$, $g_x = g_y = 2{\cdot}040 \pm 0{\cdot}005$, $g_y = 2{\cdot}303 \pm 0{\cdot}005$, $A_x = A_y = 0{\cdot}001$, $A_z = 0{\cdot}014$ cm^{-1} ($\Delta M = 2$) and $A_z = 0{\cdot}016$ cm^{-1} ($\Delta M = 1$), $W_x = W_y = W_z = 8$ G ($\Delta M = 2$) and $W_x = W_y = 24$ G and $W_z = 15$ G ($\Delta M = 1$), $J = +30$ cm^{-1}

1 : 9 ratio. The results are shown in Figure 7 and agree very well with those reported by Hatfield *et al.*[24] Much

[22] D. E. Sands, 'Introduction to Crystallography,' W. A. Benjamin, *New York*, 1969, p. 9.

[23] S. Scarnicar and B. Matkovic, *Chem. Comm.*, 1967, 297; *Acta Cryst.*, 1969, **B25**, 2046.

[24] W. E. Hatfield, J. A. Barnes, D. Y. Jeter, R. Whyman, and E. R. Jones, *J. Amer. Chem. Soc.*, 1970, **92**, 4982.

of the $\Delta M = 1$ spectrum is obscured to some extent by a residual monomer spectrum, however the low field 'r' lines form a beautifully resolved seven-line pattern in the 2000—2500 G region. At 3540 G there is a very strong line which is the high field 'x' line. Computer fits were based on both $\Delta M = 1$ and $\Delta M = 2$ spectra and are shown along with the experimental results in Figure 7. It can be seen that the fits are very acceptable except that the positions of the calculated high field $\Delta M = 1$ 'r' lines are not in complete agreement with the experimental data. The simulated $\Delta M = 2$ curve, while matching peak positions extremely well, does not quite agree in overall shape with the experimental result. Increasing the linewidth did not succeed in improving the shape and in fact blotted out the resolution of the doublet lines 6 and 7 *ca.* 1500 G.

In spite of the overall excellent agreement between theory and experiment, one puzzle remains. To achieve the best results it was necessary to assume different values of A_z for $\Delta M = 1$ and $\Delta M = 2$ spectra *viz.* 0·016 ($\Delta M = 1$) and 0·014 cm^{-1} ($\Delta M = 2$).

Comparison of the *X*-ray and e.s.r. results for ξ and r shows excellent agreement indicating that the copper(II) dimers in bis(pyridine *N*-oxide)zinc(II) nitrate are very much the same as in bis(pyridine *N*-oxide)copper(II) nitrate. The results are summarised in Table 3. Thus the doping of the copper(II) complex into the corresponding zinc complexes has little effect on the structure of the copper complex. This example clearly provides an excellent test case to provide adequate justification for the determination of the copper(II)–copper(II) separation, r, and orientational parameters, *e.g.* ξ, on the basis of a dipole–dipole coupled model. And this in a case for which $J = +30$ cm^{-1}!

So we conclude that even when J is as large as $+30$ cm^{-1}, there seems to be no ground for using the Bleeney–Bowers relation [5] to predict a pseudo-dipolar contribution to the triplet state splitting. That this is a sensible conclusion is based on the observation that in this case with $J > 0$, dipole–dipole and pseudo-dipolar splittings will have the same sign! Thus in view of the fact that 'D' from e.s.r. leads to an exact match with the *X*-ray internuclear separation of the copper(II) ions in the pure compound on the basis of dipole–dipole coupling alone, there can be no contribution to 'D' from the Bleaney and Bowers [5] type of interaction. If on the other hand J were negative, we could conceivably have a pseudo-dipolar contribution of twice the magnitude of the dipole–dipole term, but of opposite sign. This unusual situation has more or less occurred before,[3] in a system where J *ca.* -200 cm^{-1}, but it should not be relevant for the present system.

The use of the Bleaney and Bowers [5] result for the pseudo-dipolar splitting of the ground state has never been justified when exchange coupling in the ground state is weak. So it ought perhaps not be used to estimate J from a value of D. At best it may give an indication of the magnitude of D when J is known. Chasteen and Belford point out in an addendum and correction to their paper on copper(II) tartrate,[12b] that the Bleaney and Bowers [5] formula should probably involve the use of the smaller excited state exchange integrals, which certainly fits in with our conclusions. Ross and Yates [8] pointed out many years ago that it is likely that the Bleaney–Bowers formula should be replaced by a new one which includes at least two exchange integrals.

Bis(salicylaldehydato)copper(II).—The crystal structure of bis(salicylaldehydato)copper(II) shows that although the co-ordination is basically planar, weak axial interactions with neighbouring molecules occurs.[25,26] Three crystal modifications have been noted, the structure of two of which have been studied by *X*-ray crystallography. On recrystallisation from hot ethanol the modification containing the dimeric form where the bonding between neighbouring molecules occurs through the oxygen atoms was obtained. In this form each ligand is essentially planar but their two planes are separated within the complex by 0·37 Å. The perpendicular distance from a copper atom to the plane of the neighbouring chelate ring is 3·13 Å, which is slightly shorter than the distance to the oxygen atom so that the interaction may be with a delocalised system rather than with a specific atom. The angle of tilt differs in the two forms such that the copper(II) atom makes its closest contact with a different delocalised system in each. The molecules in each form are distorted but not in the same way.

We deduced $r' = 4{\cdot}05$ Å and $\xi' = 28°$ from the *X*-ray data. This form is shown schematically in

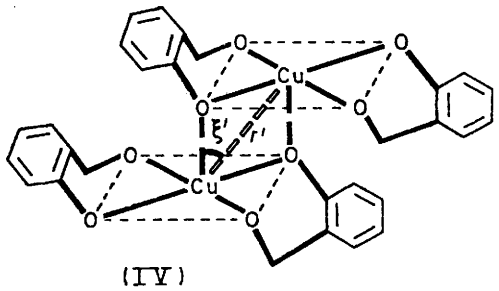

(IV)

structure (IV). In the dimeric form obtained by crystallisation from cold chloroform, the *X*-ray data led to values of $r' = 6{\cdot}4$ Å and ξ' *ca.* 60°.[22] Magnetic susceptibility measurements carried out many years ago by Calvin and Barkelew [27] showed that the magnetic moment was normal down to 100 K. If there is any exchange coupling at all, it should be quite small.

E.S.R. Results.—The e.s.r. results shown in Figure 8 were obtained at *X*-band frequency and at 77 K using a frozen saturated solution of bis(salicylaldehydato)-copper(II) in chloroform containing 20% by volume of toluene. There is a well resolved $\Delta M = 2$ spectrum

[25] D. Hall, A. J. McKinnon, and T. N. Waters, *J. Chem. Soc.*, 1965, 425.

[26] D. Hall, A. J. McKinnon, and T. N. Waters, *J. Chem. Soc.*, 1964, 3290.

[27] M. Calvin and C. H. Barkelew, *J. Amer. Chem. Soc.*, 1946, **68**, 2267.

but unfortunately insufficient spectrometer sensitivity to resolve any of the $\Delta M = 1$ lines from the residual monomer spectrum [Figure 8(b)].

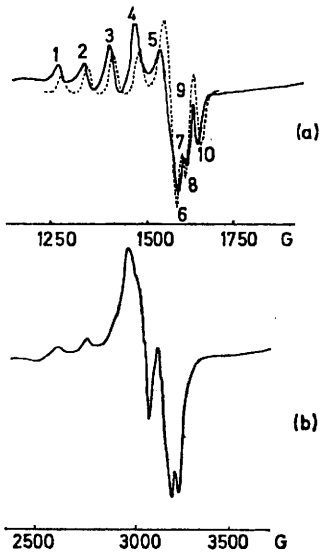

FIGURE 8 *X*-Band e.s.r. spectrum due to a solution of bis(salicylaldehydato)copper(II) in chloroform containing 20% by volume of toluene. Microwave frequency 9083 MHz, temperature 77 K —— (a) $\Delta M = 2$ dimer spectrum (b) monomer spectrum; $\Delta M = 1$ dimer lines not observed. Computer simulated $\Delta M = 2$ spectrum – – – – obtained with following parameters: $r = 4{\cdot}05 \pm 0{\cdot}05$ Å, $\xi = 30 \pm 2°$, $A_x = A_y = 0{\cdot}001$ cm^{-1}, $A_z = 0{\cdot}0150 \pm 0{\cdot}0050$ cm^{-1}, $g_x = g_y = 2{\cdot}025 \pm 0{\cdot}005$, $g_z = 2{\cdot}265 \pm 0{\cdot}050$, $W_x = W_y = W_z = 10$ G. Value of J not known and not important in simulating $\Delta M = 2$ spectrum

Computer simulation of the $\Delta M = 2$ spectrum agreed with experiment only for r *ca.* 4·05 and ξ *ca.* 30° and not for the alternative possibility r *ca.* 6·4 Å and ξ *ca.* 60°. From this we may conclude that the dimer in the frozen solution is closely similar to that in the solid crystallised from hot ethanol solution and not that from cold chloroform solutions. E.s.r. details are given in Figure 8 and the structural data summarised in Table 3.

Copper Tartrate, $Na_2Cu[(\pm)\text{-}C_4O_6H_2],5H_2O$.—A recent crystal structure determination of the complex

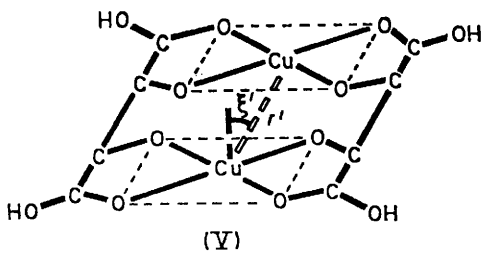

(V)

$Na_2Cu[(\pm)\text{-}C_4O_6H_2],5H_2O$ [28] has shown that the structure exists as centrosymmetric dimers with a copper(II)–copper(II) distance of $r' = 2{\cdot}986$ Å. In agreement with Belford *et al.*[28] we deduce that $\xi' = 31°$. This form is represented schematically by structure (V). In addition these authors carried out magnetic susceptibility measurements showing that $J = -18$ cm^{-1} and that therefore the singlet is lowest in energy.

The e.s.r. spectrum of disodium copper tartrate has been described previously [12,28] and found to provide evidence for the presence of triplet state phenomena. A semi-empirical approach was used to extract useful structural information about the dimeric species. We have repeated the e.s.r. of this system so as to be able to simulate the spectrum and obtain a more satisfactory interpretation for the data.

There is also structural information available now for pure copper(II) *meso* (or *l*—) tartrate and copper(II) *d*-tartrate, showing that the structure of the dimeric form depends markedly on the iosmeric form of the tartrate.[29] The complex obtained from the *meso* form is orthorhombic involving copper(II) ions joined into chains by chelate linkages from the hydroxo- and carboxo-oxygen atoms such that the internuclear copper(II)–copper(II) ion separation is 6·065 Å. The complex formed from the *d*-form of the tartrate is monoclinic with two crystallographically independent copper(II) ions in an asymmetric unit linked together by two similarly independent tartrate groups to form the dimeric complex where the internuclear separation is 5·42 Å. We have not attempted to carry out e.s.r. measurements on these compounds.

E.S.R. Results.—The preparation of the solutions of $Na_2Cu[(\pm)\text{-}C_4O_6H_2],5H_2O$ in ethylene glycol–water solution was carried out as in the work of Chasteen and Belford.[12] E.s.r. spectra at *X*-band were recorded at 77 K and are reproduced in Figure 9 showing excellent agreement with those reported by Chasteen and Belford.[12] Both $\Delta M = 1$ and $\Delta M = 2$ spectra are well resolved, and provide a further excellent opportunity to test our method of approach to the use of e.s.r. It can be seen in Figure 9 that the best fit simulated spectra match the experimental result extremely well.

The peaks on the $\Delta M = 2$ experimental and simulated spectra match within ± 4 G in all cases except (10) at 1577 G, which comes out 10 G too low in the calculated spectrum. Using the same parameters as for the $\Delta M = 2$ spectra, the $\Delta M = 1$ spectrum shown in Figure 9 was obtained. The two large peaks, arising from molecules aligned with H in the *xy* plane at *ca.* 2800 and *ca.* 3400 G, do not have quite the correct positions. The 'r' lines in the range 2000—2500 G and those *ca.* 3500 G fit easily to within *ca.* 20 G. Attempts to refine the $\Delta M = 1$ fit any further were not fruitful. It is very interesting to note the presence of a group of lines shown at high gain *ca.* 3200 G, which were also observed by Chasteen and Belford.[12] These actually occur in the computed spectrum, and are thought to arise from those molecules for which H lies in the *zy* plane at an angle *ca.* $\xi + 90°$ from the *z*-axis.

We can, therefore, account very satisfactorily for all

[28] R. L. Belford, R. J. Missavage, I. C. Paul, N. D. Chasteen, W. E. Hatfield, and J. F. Villa, *Chem. Comm.*, 1971, 508.

[29] C. K. Prout, J. R. Carruthers, and F. J. C. Rossotti, *J. Chem. Soc.* (*A*), 1971, 3336.

features of the experimental spectrum, though in minor detail we experience some limitations to second order perturbation theory. From the e.s.r. results we conclude that $r = 3{\cdot}77 \pm 0{\cdot}05$ Å and $\xi = 29 \pm 1°$. Chasteen and Belford [12] interpreted their results semi-empirically and obtained a point dipole value of $r = 3{\cdot}8$ Å. It is easy to see that the value of r is considerably larger than $r' = 2{\cdot}986$ Å obtained from X-ray

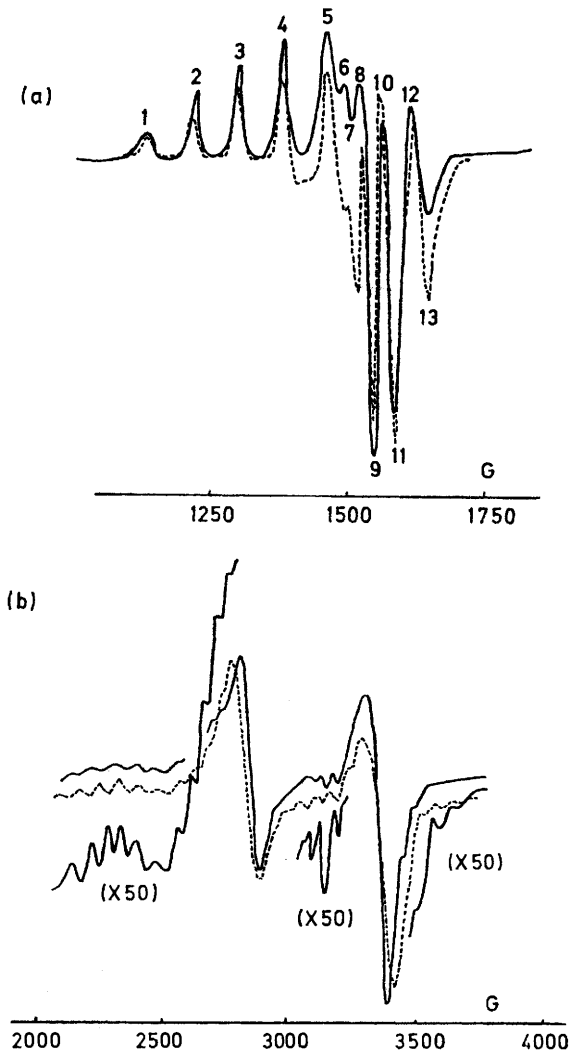

FIGURE 9 X-Band e.s.r. spectrum due to 0·2M solution of $Na_2Cu[(\pm)\text{-}C_4O_6H_2],5H_2O$ in ethylene glycol–water. Microwave frequency 9081 MHz, temperature 77 K —— (a) $\Delta M = 2$ spectrum, (b) $\Delta M = 1$ spectrum. Computer simulated spectra – – – – obtained with following parameters: $r = 3{\cdot}77 \pm 0{\cdot}05$ Å, $\xi = 29 \pm 1°$, $g_x = g_y = 2{\cdot}060 \pm 0{\cdot}005$, $g_z = 2{\cdot}278 \pm 0{\cdot}008$, $A_x = A_y = 0{\cdot}003$, $A_z = 0{\cdot}0178 \pm 0{\cdot}0010$ cm^{-1}, $W_x = W_y = W_z = 8$ G ($\Delta M = 2$), 18 G ($\Delta M = 1$), $J = -18$ cm^{-1}

studies [28] however ξ and ξ' agree within 1°. Chasteen and Belford, noting this apparent discrepancy, sought to reduce their value of r first by including covalency and, secondly, by considering the effect of a distributed magnetic moment. Even then they were not able to arrive at a value as low as 2·99 Å for r! We conclude that the dimer structure in the solvent is not the same as that in the pure compound. There is certainly no reason *a priori* to believe that it must be. The results are summarised in Table 3 and in the caption to Figure 9.

TABLE 3

Comparison of e.s.r. and X-ray * structural data †

Complex	E.s.r. r/Å	E.s.r. ξ^0	X-Ray r'/Å	X-Ray ξ'^0
Copper(II) diethyldithiocarbamate	3·85 ±0·05	42 ± 2	3·58	41
Zinc(II) diethyldithiocarbamate			3·54	
Zinc(II) dimethyldithiocarbamate			3·97	
Bis(pyridine N-oxide)copper(II) nitrate	3·46 ±0·05	41 ± 1	3·46	41
Bis(salicylaldehydato)copper(II)	4·05 ±0·05	30 ± 2	4·05	28
Copper(II) tartrate	3·77 ±0·05	29 ± 1	2·99	31

* ξ' and r' Based on X-ray data from the pure compound in each case. † See text for details and references.

CONCLUSION

We have presented the relevant theory to account for the e.s.r. spectra of a certain class of low symmetry copper(II) dimers whose structure was known, or suggested, by X-ray crystallographic data. In turn we have described the computer simulation of the spectra and have compared theoretical and experimental results.

The theory is basically a little more general than required to deal with the actual results presented, however it is given in full since both small J and large J cases can be treated in much the same way. Others who may wish to analyse similar spectra should find our results useful. A little modification to the theory will enable cases where the dimers are not centrosymmetric to be treated.

Bis(pyridine N-oxide)copper(II) nitrate doped into the isomorphous zinc host appears to have the same dimer structure as in the pure copper compound. The values of $r = 3{\cdot}45$ Å and $\xi = 41°$ are in almost exact agreement with the X-ray results for the pure copper system. This result is helpful from another point of view. The excellent agreement between structural data from e.s.r., based on a pure dipolar model alone, coupled with fact that $J = +30$ cm^{-1}, indicates very strongly that no pseudo dipolar contribution to the triplet state energy splitting occurs. Therefore considerable caution seems necessary in the application of formula of the Bleaney and Bowers [5] type to this kind of problem.

The example of copper(II) diethyldithiocarbamate diluted in the zinc host is interesting for several reasons. First of all the value of $r = 3{\cdot}85$ Å is somewhat larger than $r' = 3{\cdot}58$ Å for the pure copper compound, and the zinc–zinc distance in the zinc host, where $r' = 3{\cdot}54$ Å, as determined by X-ray methods. That observation, as well as the negative result from e.s.r. measurements

on copper(II) doped into the nickel compound, which does not have dimeric structure, suggests very strongly that the host compound exerts the determining influence in the behaviour of copper(II) ions present in moderate concentrations in other metal thiocarbamates. Secondly, the occurrence of three distinct g values and hyperfine constants for isolated copper(II) ions in zinc diethyldithiocarbamate gave the opportunity to consider whether the copper(II)–copper(II) dimers perhaps had triclinic symmetry (see Table 1). We found no evidence for this. The g-values are very close to 2, much closer than for most other copper complexes. Recently Keijzers *et al.*[30] have carried out simplified Hückel type calculations on this system and showed good agreement with experimental g-values. We are unable to account at present for the smaller g-values required in fitting the dimer spectra than those reported by Weeks and Fackler.[20]

Previously we had found that a dimeric form of copper(II) diethyldithiocarbamate can exist in frozen solutions of the chelate in certain mixtures of organic solvents. The results were interpreted in terms of an axial model and showed a much longer copper(II)–copper(II) distance of *ca.* 4·5 Å.[19]

As far as we can tell, the structure of the frozen solution of dimer of bis(salicylaldehydato)copper(II) in chloroform–toluene is the same as that of the pure compound. Although J is not known, but is probably very small indeed, its precise value is not important in connection with the $\Delta M = 2$ spectrum which was the only part of the dimer spectrum identified.

[30] C. P. Keijzers, H. J. M. DeVries, and A. van der Avoird, *Inorg. Chem.*, 1972, **11**, 1338.

For disodium copper(II) tartrate, we are left with the conclusion that the dimer structure in frozen solutions of ethyleneglycol–water is different from that in the pure compounds.

In all cases, g-values and hyperfine constants deduced from the dimer simulated spectra are in general agreement with available evidence for monomers of the same system, or in accord with what might be expected.

EXPERIMENTAL

E.s.r. measurements were recorded as previously described [12] at 77 and 293 K using a Varian 100 kHz multipurpose cavity and a spectrometer of conventional design.

APPENDIX

Hyperfine Coefficients τ_1—τ_5 [*see equations* (8) *and* (9)].—

$$\begin{aligned}
\tau_1 &= A_z A_\perp / K \\
\tau_2 &= A_x A_y / A_\perp \\
\tau_3 &= [A_z(A_y^2 - A_x^2) g_x g_y g_z \sin\phi \cos\phi \cos\theta]/(KgA_\perp g_\perp^2) \\
\tau_4 &= g_z g_\perp (A_\perp^2 - A_z^2) \sin\theta \cos\theta/(Kg^2) \\
\tau_5 &= \tau_3 A_\perp g_\perp \tan\theta/(A_z g_z)
\end{aligned} \tag{A1}$$

Relationships between ψ, ψ', γ, γ' *and* θ, ϕ

$$\begin{aligned}
\cos\psi &= g_z \cos\theta/g \\
\sin\psi &= g_\perp \sin\theta/g \\
\cos\psi' &= g_x \cos\phi/g_\perp \\
\sin\psi' &= g_y \sin\phi/g_\perp
\end{aligned} \tag{A2}$$

$$\begin{aligned}
\cos\gamma &= A_z g_z \cos\theta/Kg \\
\sin\gamma &= A_\perp g_\perp \sin\theta/Kg \\
\cos\gamma' &= A_x g_x \cos\phi/A_\perp g_\perp \\
\sin\gamma' &= A_y g_y \sin\phi/A_\perp g_\perp
\end{aligned} \tag{A3}$$

The Energy Matrix.—Uncoupled representation.

	$\lvert{+}{+}m_1m_2\rangle$ $\lvert\psi_1\rangle$	$\lvert{+}{-}m_1m_2\rangle$	$\lvert{-}{+}m_1m_2\rangle$	$\lvert{-}{-}m_1m_2\rangle$ $\lvert\psi_3\rangle$
$\langle{+}{+}m_1m_2\rvert$	$g\beta H + D_{zz}'/4 + \frac{1}{2}K(m_1 + m_2)$	$G_1^* + \frac{1}{2}(\tau_4 - i\tau_5)m_2$	$G_2^* + \frac{1}{2}(\tau_4 - i\tau_5)m_1$	G_3^*
$\langle{+}{-}m_1m_2\rvert$	c.c.	$-D_{zz}'/4 + \frac{1}{2}K(m_1 - m_2)$	$G_4^* - \frac{1}{2}J$	$-G_2^* + \frac{1}{2}(\tau_4 - i\tau_5)m_1$
$\langle{-}{+}m_1m_2\rvert$	c.c.	c.c.	$D_{zz}'/4 - \frac{1}{2}K(m_1 - m_2)$	$-G_1^* + \frac{1}{2}(\tau_4 - i\tau_5)m_2$
$\langle{-}{-}m_1m_2\rvert$	c.c.	c.c.	c.c.	$-g\beta H + D_{zz}'/4 - \frac{1}{2}K(m_1 + m_2)$

(A4)

c.c. denotes complex conjugate

$$\begin{aligned}
G_1 &= \frac{1}{4}(D_{zx} + iD_{zy}) \\
G_2 &= \frac{1}{4}(D_{xz} + iD_{yz}) \\
G_3 &= \frac{1}{4}(D_{xx} - D_{yy}) + \frac{i}{4}(D_{xy} + D_{yx}) \\
G_4 &= \frac{1}{4}(D_{xx} + D_{yy}) + \frac{i}{4}(D_{yx} - D_{xy}) = D_2 - iD_6
\end{aligned} \tag{A5}$$

(see eqn. 14)

Coupled representation [*see equation* (15) *for definitions of* $|\psi_1\rangle$].

	$\|\psi_1\rangle$ $\|++m_1m_2\rangle$	$\|\psi_2\rangle$	$\|\psi_3\rangle$ $\|--m_1m_2\rangle$	$\|\psi_4\rangle$
$\langle\psi_1\|$	$g\beta H + D_{zz}'/4 + \frac{1}{2}K(m_1+m_2)$	$S_1 + iS_2$	$S_3 + iS_4$	$S_7 + iS_8$
$\langle\psi_2\|$	c.c.	$-D_{zz}'/4 + \Phi$	$S_5 + iS_6$	0
$\langle\psi_3\|$	c.c.	c.c.	$-g\beta H + D_{zz}'/4 - \frac{1}{2}K(m_1+m_2)$	$S_9 + iS_{10}$ $S_9 + iS_{10}$
$\langle\psi_4\|$	c.c.	c.c.	c.c.	$-D_{zz}'/4 - \Phi$

(A6)

$$\Phi = [D_2'^2 + D_6^2 + \tfrac{1}{4}K^2(m_1 - m_2)^2]^{\frac{1}{2}},\ (D_2' = D_2 - \tfrac{1}{2}J) \tag{A7}$$

U, V, b, W, X, and d required to define $|\psi_2\rangle$ and $|\psi_4\rangle$ are defined as:

$$\begin{aligned} U &= D_2'/f_1,\ V = -D_6/f,\ b = [\Phi - \tfrac{1}{2}K(m_1 - m_2)]/f_1 \\ f_1 &= \{D_2'^2 + D_6^2 + [\Phi - \tfrac{1}{2}K(m_1 - m_2)]^2\}^{\frac{1}{2}} \\ W &= D_2'/f_2,\ X = -D_6/f_2,\ d = [-\Phi - \tfrac{1}{2}K(m_1 - m_2)]/f_2 \\ f_2 &= \{D_2' + D_6^2 + [-\Phi - \tfrac{1}{2}K(m_1 - m_2)]^2\}^{\frac{1}{2}} \end{aligned} \tag{A8}$$

The S_i are defined as follows.

$$\begin{aligned}
S_1 &= (UD_{zx} + VD_{zy} + bD_{xz})/4 + [(U\tau_4 + V\tau_5)m_2 + b\tau_4 m_1]/2 \\
S_2 &= (VD_{zx} - UD_{zy} - bD_{yz})/4 + [(-U\tau_5 + V\tau_4)m_2 - b\tau_5 m_1]/2 \\
S_3 &= (D_{xx} - D_{yy})/4 = D_3 \\
S_4 &= -(D_{xy} + D_{yx})/4 \\
S_5 &= (-UD_{xz} + VD_{yz} - bD_{zz})/4 + [(U\tau_4 - V\tau_5)m_1 + b\tau_4 m_2]/2 \\
S_6 &= (VD_{xz} + UD_{yx} + bD_{zy})/4 - [(V\tau_4 + U\tau_5)m_1 + b\tau_5 m_2]/2 \\
S_7 &= (WD_{zx} + XD_{zy} + dD_{xz})/4 + [(W\tau_4 + X\tau_5)m_2 + d\tau_4 m_1]/2 \\
S_8 &= (XD_{zx} - WD_{zy} - dD_{yz})/4 + [(-W\tau_5 + X\tau_4)m_2 - d\tau_5 m_1]/2 \\
S_9 &= (-WD_{xz} + XD_{yz} - dD_{zz})/4 + [(W\tau_4 - X\tau_5)m_1 + d\tau_4 m_2]/2 \\
S_{10} &= (-XD_{xz} - WD_{yz} - dD_{zy})/4 + [(W\tau_5 + X\tau_4)m_1 + d\tau_5 m_2]/2
\end{aligned} \tag{A9}$$

Although $V = X = 0$ in this case since $D_6 = 0$, we leave V and X in equations (A9) for then the expressions for S_i are in the most general form, and could be applied to more complicated cases.

Energy Levels and Wavefunctions.—2nd Order perturbation Theory. The energy levels to second order in $\mathcal{H}_d$, J, and the hyperfine interaction are given by:

$$\begin{aligned}
E_1 &= g\beta H + D_{zz}'/4 + \tfrac{1}{2}K(m_1 + m_2) + (S_1^2 + S_2^2)/\Delta_{12}^0 + (S_3^2 + S_4^2)/\Delta_{13}^0 + (S_7^2 + S_8^2)/\Delta_{14}^0 \\
E_2 &= -D_{zz}'/4 + \Phi - (S_1 + S_2)/\Delta_{12}^0 + (S_5^2 + S_6^2)/\Delta_{23}^0 \\
E_3 &= -g\beta H + D_{zz}'/4 - \tfrac{1}{2}K(m_1 + m_2) - (S_3^2 + S_4^2)/\Delta_{13}^0 - (S_5^2 + S_6^2)/\Delta_{23}^0 - (S_9^2 + S_{10}^2)/\Delta_{43}^0 \\
E_4 &= -D_{zz}'/4 - \Phi - (S_7^2 + S_8^2)/\Delta_{14}^0 + (S_9^2 + S_{10}^2)/\Delta_{43}^0
\end{aligned} \tag{A10}$$

The wavefunctions to first order, apart from small normalisation factors are

$$\begin{aligned}
|\psi_1\rangle' &= |\psi_1\rangle + (S_1 - iS_2)/\Delta_{12}^0|\psi_2\rangle + (S_3 - iS_4)/\Delta_{13}^0|\psi_3\rangle + (S_7 - iS_8)/\Delta_{14}^0|\psi_4\rangle \\
|\psi_2\rangle' &= |\psi_2\rangle - (S_1 + iS_2)/\Delta_{12}^0|\psi_2\rangle + (S_5 - iS_6)/\Delta_{23}^0|\psi_3\rangle \\
|\psi_3\rangle' &= |\psi_3\rangle - (S_3 + iS_4)/\Delta_{13}^0|\psi_2\rangle - (S_5 + iS_6)/\Delta_{23}^0|\psi_2\rangle - (S_9 - iS_{10})/\Delta_{43}^0|\psi_4\rangle \\
|\psi_4\rangle' &= |\psi_4\rangle - (S_7 + iS_8)/\Delta_{14}^0|\psi_1\rangle + (S_9 + iS_{10})/\Delta_{43}^0|\psi_3\rangle
\end{aligned} \tag{A11}$$

Δ_{ij}^0 are the zero order energy differences between states i and j.

Second order energy shifts due to τ_1—τ_3 *terms in equation* (8).

$$\begin{aligned}
\Delta E_1 &= \{\tfrac{1}{2}[2I(I+1) - m_1^2 - m_2^2](\tau_1^2 + \tau_2^2 + \tau_3^2) - \tau_1\tau_2(m_1 + m_2)\}/4\Delta^0 \\
\Delta E_2 &= \{\tfrac{1}{2}(a^2 - b^2)(m_2^2 - m_1^2)(\tau_1^2 + \tau_2^2 + \tau_3^2) - \tau_1\tau_2(m_1 + m_2)\}/4\Delta^0 \\
\Delta E_3 &= \{-\tfrac{1}{2}[2I(I+1) - m_1^2 - m_2^2](\tau_1^2 + \tau_2^2 + \tau_3^2) - \tau_1\tau_2(m_1 + m_2)\}/4\Delta^0 \\
\Delta E_4 &= \{-\tfrac{1}{2}(a^2 - b^2)(m_2^2 - m_1^2)(\tau_1^2 + \tau_2^2 + \tau_3^2) - \tau_1\tau_2(m_1 + m_1)\}/4\Delta^0
\end{aligned} \tag{A12}$$

Special Case $|J| \approx h\nu \approx g\beta H_0$.—Suppose that $J = -h\nu$. In this case it is more correct to take the zero order energies as arising not from the Zeeman interaction alone, but Zeeman and exchange together. Then $\Delta_{14}^0 \simeq 2g\beta H_0$ and $\Delta_{43}^0 \simeq 0$. Then it is not correct to use the energy expressions in equations (A10) as they stand. Another way of putting this is to say that states $|\psi_3\rangle$ and $|\psi_4\rangle$ are not close to being eigenstates of the system. Therefore we may explore the implications of this dilemma by diagonalising the 2×2 matrix involving states $|\psi_3\rangle$ and $|\psi_4\rangle$. And then binomial expansions may be used to approximate the energies when $|J| < h\nu$ and $|J| > h\nu$. So in this way the likely effects of $|J| \simeq h\nu$ can be obtained without recourse to diagonalisation of the total 64×64 matrix.

The energy matrix is then worked out in the modified basis, and second order perturbation theory employed as before. Although we cannot be sure of the complete reliability of the preliminary computer simulations obtained, it seems clear that the spectrum is quite different from that when $|J| \ll h\nu$ or $|J| \gg h\nu$. This matter will be investigated further in detail only if appropriate practical examples which require such a treatment arise.

The Australian Research Grants Committee is thanked for continued financial support. P. D. W. B. acknowledges receipt of a Commonwealth post-graduate award and A. D. T. acknowledges receipt of a Monash graduate scholarship.

[2/2334 *Received*, 12*th October*, 1972]